Frontiers in Bioscience Landmark

Front. Biosci. (Landmark Ed) **2022**; 27(11): 307
https://doi.org/10.31083/j.fbl2711307

Original Research

A Promising Target of Langchuangding Prescription Treating Systemic Lupus Erythaematosus Integrated Network Pharmacology with HPLC-MS and Molecular Docking

Qianqian Li[1,†], Jing Sun[2,†], Jifang Tu[3], Haichang Li[3], Jida Zhang[3], Huanpeng Gu[3], Zhijun Xie[3,*], Huiqing Lv[1,*]

[1]School of Pharmaceutical Sciences, Zhejiang Chinese Medical University, 311402 Hangzhou, Zhejiang, China
[2]The Second School of Clinical Medicine, Zhejiang Chinese Medical University, 310053 Hangzhou, Zhejiang, China
[3]School of Basic Medical Sciences, Zhejiang Chinese Medical University, 310053 Hangzhou, Zhejiang, China
*Correspondence: xzj575@163.com (Zhijun Xie); lvhuiqing@zcmu.edu.cn (Huiqing Lv)
[†]These authors contributed equally.
Academic Editor: Fazle Elahi
Submitted: 17 June 2022 Revised: 13 September 2022 Accepted: 14 October 2022 Published: 15 November 2022

Abstract

Background: Systemic lupus erythematosus (SLE) is a chronic multisystem autoimmune disorder affecting almost any organ system without effective treatment. Based on accumulating evidence, activated T cells are key cause promoting the pathogenesis of SLE. A traditional clinic Langchuangding formula (LCD) is an effective clinical traditional Chinese medicine prescription for SLE with few side effects and good patient compliance. However, the mechanism of how LCD affects SLE remains unclear. **Methods**: Targets related to LCD and SLE were predicted and overlapped to construct protein-protein interaction (PPI) for screening core target. Subsequently, flow cytometry analysis and Western-blot method were used to verify the expression levels of target gene in LCD serum treated-Jurkat T cells. The main compounds of LCD were identified by HPLC-MS and further docked with the core targe. **Results**: 283 protein targets in LCD, 1498 SLE targets and 150 common targets were obtained to construct protein-protein interaction (PPI). Network pharmacology results suggested that LCD was closely related to CASP3 target. To verify the prediction of pharmacological mechanism of LCD treatment for SLE, we investigated the anti-proliferative effects of LCD-treated rat serum on β-oestradiol (300 pg/mL)-activated Jurkat T cells *in vitro* using a CCK-8 kit and flow cytometry analysis and then analyzed the CASP3 expression levels. Vitro experiments confirmed that LCD serum could suppress the proliferation ($p < 0.05$) and induce apoptosis of the activated T cells through up-regulating CASP3 expression levels. Interactions between CASP3 target and LCD were further validated integrating HPLC-MS analysis and molecular docking. **Conclusions**: The results showed that LCD could relieve SLE, which might be attributed to inducing the activated T cells apoptosis by up-regulating CASP3 expression levels. The network pharmacology and molecular docking approach provide a new insight for deepening understanding about TCM. LCD potentially represents a promising therapeutic prescription for SLE supplement treatment with no adverse effects.

Keywords: systemic lupus erythaematosus; Langchuangding prescription; target; T cell apoptosis; network pharmacology; HPLC-MS

1. Introduction

Systemic lupus erythaematosus (SLE) is a multisystem autoimmune disease that involves the skin, joints, tendons, kidneys and various other organs. It is characterized by overproduction of autoantibodies, immune complex deposition and activated T cells, causing excessive inflammation and damage [1,2]. Uncontrolled T-cell activation plays key roles in the pathogenesis of SLE by promoting pro-inflammatory cytokine release and impairing the clearance of apoptotic cells [3–5]. The course of SLE is variable and unpredictable. Most patients with SLE require long-term treatment with glucocorticoids and immune-modulators. However, serious side effects occur, including central obesity, moon face, and buffalo hump [6–8]. Despite great progress in medical technology, the treatment of SLE is still a problem to be solved [9]. Traditional Chinese medicine (TCM) is a key component of complementary and alternative medicine that has been in China over a few millennia and has been increasingly integrated into conventional treatments, particularly for chronic autoimmune diseases such as SLE [10,11].

Based on the basic theory of TCM, our team proposed the Langchuangding prescription (LCD) for SLE treatment [12,13]. LCD consists of *Cimicifugae Rhizoma, Paeoniae Radix rubra, Rehmanniae Radix, Trionycis Carapax*, etc. As shown in our previous study, LCD, an effective prescription, exerts definite effects on treating SLE with fewer side effects and good patient compliance than conventional drugs such as corticosteroids and immune inhibitors [13]. However, the underlying therapeutic mechanism of LCD in treating SLE remains unclear.

Network pharmacology is a promising approach to explore the mechanism TCM formulae, which could pro-

vide a potential "network target" on a global level [14,15]. It also could reveal the complicated relationship between herbs and diseases by constructing protein-protein interaction (PPI) networks [16,17]. However, the accuracy of the network pharmacology analysis results remains limited due to lack of unified standards. Due to the multi-components and multi-targets of TCM, we should integrate multiple systems such as high-performance liquid chromatography tandem mass spectrometry (HPLC-MS) and molecular docking to investigate the interactions of targets and its active ingredients. Moreover, *in vitro* or *vivo* experiments were performed to validate the results [14,18].

Here, in the present study, we predicted the potential mechanism of LCD treating SLE based on network pharmacology. The target of LCD for treating SLE was further predicted integrating HPLC-MS with molecular docking. To verify the target of LCD in the treatment of SLE, we prepared different doses of LCD-treated rat serum and then investigated their effects on activated Jurkat T cells by β-oestradiol (300 pg/mL) *in vitro* using flow cytometry analysis, Real-time PCR and Western blotting method. The flow chart of this study is presented in Graphical Abstract.

2. Materials and Methods

2.1 Reagents and Chemicals

HPLC-grade acetonitrile (CH3CN) and methanol were purchased from Sigma-Aldrich (St. Louis, MO, USA), while analytical grade formic acid was obtained from Huadong Chemical Reagent Co. Ltd. (Hangzhou, China). Deionized water was purified using a Milli-Q system (Millipore, Bedford, MA, USA). Other reagents were of analytical grade.

Ferulic acid (LOT#110773-200611, purity greater than 99.0%) and isoferulic acid (LOT#11698-200602, purity greater than 99.0%) were purchased from the National Institute for the Control of Pharmaceutical and Biological Products (Beijing, China). Antibodies against Caspase-3 (CASP3) and β-actin were purchased from Cell Signaling Technology (Danvers, MA, USA). The RNA isolation kit was obtained from Bio-Rad (cat# 163-2098, Bio-Rad, Hercules, CA, USA).

2.2 Materials

LCD is composed of several medicinal herbs (Table 1) that were identified by Kong-long Chen and obtained from Medical Pieces Co., Ltd., Zhejiang Chinese Medical University (Hangzhou, Zhejiang, China). All herbs were soaked in distilled water for 1 h and extracted twice with distilled water under reflux for 2 h. The filtered extracts were concentrated to a condensed LCD decoction using a rotary evaporator at 50 °C and stored at 4 °C until use.

Table 1. LCD formula.

Herb	Part used	Dosage used
Radix Rehmanniae (Shu Di Huang)	Root	15 g
Trionycis carapax (Zhi Bie Jia)	Turtle	12 g
Herba Artemisia annua (Qing Hao)	Herb	12 g
Herba Hedyotis Diffusae (She Cao)	Herb	15 g
Radix Paeoniae rubra (Chi Shao)	Root	15 g
Herba Centellae asiaticae (Ji Xue Cao)	Herb	12 g
Semen Coicis (Mi Ren)	Seed	15 g
Citri sarcodactylis (Fo Shou) fructus	Fruit	9 g
Rhizoma Cimicifugae (Sheng Ma)	Rhizome	9 g
Radix Glycyrrhizae (Gan Cao)	Root	6 g

2.3 Prediction of Potential Mechanism of LCD Treating SLE

Potential targets from LCD and related SLE disease were obtained from 5 kinds of database such as TCMSP (http://www.tcmsp-e.com), Genecards (https://www.genecards.org/) OMIM, TTD and Drugbank. We further used human protein-protein STRING database (https://www.string-db.org/) to construct the protein-protein interaction (PPI) networks of LCD and SLE and visualized using Cytoscape 3.7.1 (Oracle, Austin, TX, USA). The key targets were input into Webgestalt website (http://www.webgestalt.org) for the enrichment analysis of Kyoto Encyclopedia of Genes and Genomics (KEGG) pathways.

2.4 Validation of LCD Treating SLE

2.4.1 LCD-Treated Rat Serum Preparation

Animal treatment: Male Sprague-Dawley rats (300 $\pm$ 20 g body weight) were obtained from the experimental animal centre of Zhejiang Chinese Medical University [SCXK (Yu)-2005-3001], Zhejiang Province, P.R. China. The animal study was reviewed and approved by Animal Ethical and Welfare Committee of ZCMU. Animals were housed under standard conditions of temperature, humidity, and light and provided with plentiful food and water. All procedures involving animals were conducted in accordance with the regulations of experimental animal administration issued by the State Committee of Science and Technology of People's Republic of China. After a week of adaptive feeding, rats were randomly divided into control groups and three LCD-treated groups. Rats were administered LCD decoction by gavage for 3 days at high (72.6 g/kg.bw), middle (36.3 g/kg.bw) and low (18.1 g/kg.bw) doses, respectively, which is listed as grams per kilogram rat body weight, to prepare high (H), middle (M) and low (L) doses of LCD serum. The doses were based on the conversion from human to rat according to clinical application. The untreated rats were administered distilled water accordingly. The dosages were calculated based on the weight of rats, which were measured daily.

LCD serum sample preparation: Blood was collected from the orbital vein of each rat on the 3rd day 1 h after the last drug administration, allowed to clot for approximately 45 min at room temperature and then centrifuged at 3000 rpm for 10 min. The obtained LCD serum samples were prepared for analyses as follows: 400 μL of cold methanol were added to 100 μL of serum for protein precipitation, which was performed in an ice-water bath. After vortex mixing for 30 s and centrifugation at 12,000 rpm at 4 °C for 10 min, the supernatant was collected and filtered through a 0.45 μm filter and stored at –80 °C for further analysis.

2.4.2 Analysis of Main Components in LCD Serum by HPLC-MS

We integrated HPLC-MS analysis with molecular docking to further validate the interactions between CASP3 target and LCD. Different doses of LCD treated serum were prepared and identified with HPLC/MS analysis. LCD treated-rat serum were identified using an ion trap mass spectrometer equipped with an electrospray ionization (ESI) source (Thermo Fisher, USA) under the control of Xcalibur software (version 1.4, Thermo Fisher, USA) [16]. Chromatographic separation was performed using reverse-phase HPLC on a Dionex C18 column (4.6 $\times$ 250 mm id, particle size 5.0 μm). The mobile phase consisted of 0.1% formic acid (A) and acetonitrile (B) using the following 25 min gradient elution program: 0 min to 5 min, 80% A; 5 min to 10 min, 67% A; 10 min to 15 min, 66% A; and 15 min to 25 min, 60% A. The injection volume was 2 μL at a flow rate of 0.2 mL/min. The detection wavelength was set to 325 nm at a column temperature of 25 °C.

The HPLC eluents were analyzed with a mass spectrometer (Bruker, MA, USA) connected to an Ultimate 3000 HPLC system (Thermo Fisher Scientific, Wilmington, DE, USA) via an ESI interface. High purity nitrogen was used as the nebulizer and auxiliary gas, and argon was the collision gas. The Q-TOF-MS was operated in positive ion mode with a spray voltage of 4.5 KV and a collision-induced dissociation voltage of 25 V.

2.4.3 Molecular Docking Simulation

To further predict the possible component-target interaction, we used molecular docking simulation in this study. Structure information of the components was obtained from the NBCI PubChem database (https://pubchem.ncbi.nlm.nih.gov/). The three dimensional (3D) structures were optimized by Chem3D (ChemDraw Professional software 17.0, Cambridge, USA) and saved in MOL2 format. We obtained the 3D structure of protein target from the RCSB Protein Data Bank (PDB, https://www.rcsb.org/) [19] in PDB format and then used PyMOL software (Schrodinger, Inc., New York, USA) to remove water and separate ligand from the 3D protein structure. Finally, PDB format was saved as PDBQT files, further select Grid Box's range in AutoDock software and run Autodock vina (http://vina.scripps.edu/) for virtual molecular docking [20].

2.4.4 CCK-8 Cell Viability Assay

Jurkat T cell viability was evaluated using a CCK-8 assay in triplicate [21,22]. Briefly, cells (2 $\times$ 10^4 cells/well) were cultured in 96-well plates with RPMI 1640 medium (10% foetal bovine serum) in a humidified atmosphere containing 5% CO_2 at 37 °C. After adhesion, control and treated cells were treated with or without different doses of LCD serum (H, M and L) along activated with β-oestradiol (300 pg/mL) for 24 h and then incubated for 2 h with 10 μL of CCK-8 at 37 °C in the dark. After discarding cell supernatants, we detected the absorbance at 450 nm using a microplate spectrophotometer reader (Bio-Teck Instruments, Winooski, VT, USA).

2.4.5 Flow Cytometry Analysis

Jurkat cells (2 $\times$ 10^6 cells) cultured in 6-well plates were incubated with different doses of LCD serum (H, M and L) along with β-oestradiol (300 pg/mL) for 24 h. Following trypsinization, cells were washed twice with cold PBS, resuspended in binding buffer (1 $\times$ 10^6 cells/mL) and 100.0 μL of each sample were transferred to separate 5 ml tubes. Cells were stained with 5 μL of Annexin V-FITC and 15 μL of propidium iodide (20 μg/mL) and then incubated in the dark at room temperature for 15 min. The stained cells were resuspended in 400 μL of 1x binding buffer. The cells were analysed using a FACS Vantage flow cytometer with Cell Quest software (Becton Dickinson, NJ, USA). The excitation wavelength was 488 nm and the emission wavelength was 670 nm.

2.4.6 Quantitative Real-Time PCR Analysis

Expression levels of the CASP3 mRNA in T cells were analysed using quantitative real-time PCR (RT–PCR). Briefly, Jurkat cells (1 $\times$ 10^6 cells/well) cultured in 12-well plates were incubated in the absence or presence of different doses of LCD serum (H, M, and L) along with β-oestradiol (300 pg/mL) for 24 h. Then, total RNA was extracted from the cells using Trizol reagent according to the manufacturer's instructions (Invitrogen, CA, USA), and the concentration of RNA was determined using a NanoDrop 2000 spectrophotometer (Thermo Fisher Scientific, Wilmington, DE, USA). The RNA was converted to cDNAs using a cDNA Reverse Transcription Kit (Bio-Rad, CA, USA). PCR amplification of the cDNA aliquots was performed using SYBR Green PCR master mix (Bio-Rad, CA, USA). Primers for CASP3 and β-actin were synthesized by Sangon Biotech (Shanghai, China). Forward and reverse primers for CASP3 and β-actin were 5′- TGCAGACGCGGCTCCTAGCG-3′ and 5′-AACCAGAGCGCCGAGTGTGAG-3′, 5′-CGAGCACAGAGCCTCGCCTT -3′ and 5′- ACATGC-CGGAGCCGTTGTCG -3′, respectively (5′-3′ direction). Reaction was performed in PCR buffer with a total final volume of 10 μL under the following conditions: 15 s of denaturation at 94 °C, 10 s of annealing at 60 °C, and 10 s

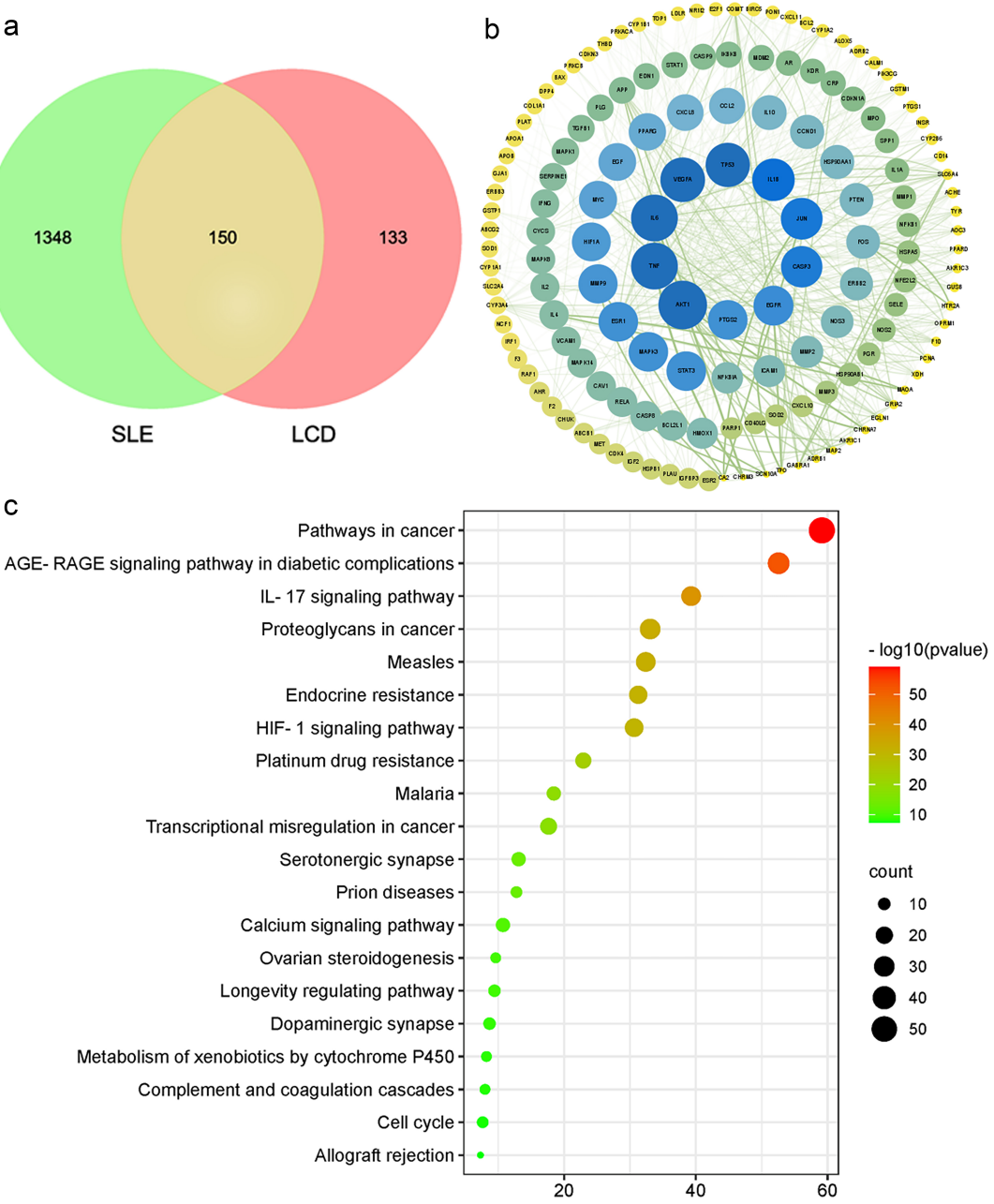

Fig. 1. Protein interactions network and KEGG pathway enrichment analysis between LCD component targets and SLE related targets. (a) Veen diagram. (b) PPI network. (c) The KEGG pathway enrichment analysis of the key targets.

elongation at 72 °C. PCR cycles were repeated 45 times. All real-time PCR experiments were run in quadruplicate. The mRNA expression levels of CASP3 were analysed using the $2^{-\Delta\Delta Ct}$ method following normalization to β-actin.

2.4.7 Western Blotting

Expression levels of the CASP3 protein were measured using western blot analysis. Briefly, Jurkat cells (1×10^6 cells/well) cultured in 12-well plates were treated with different doses of LCD serum (H, M and L) along with β-oestradiol (300 pg/mL) at 37 °C in a 5% CO_2 atmosphere. After 24 h, the cells were harvested, washed with PBS and lysed for 30 min on ice. Proteins in the lysates were quantified using a BCA protein assay kit. Subsequently, proteins (60 μg) were electrophoretically separated on 10% SDS-PAGE gels and then transferred to NC membranes. Membranes were blocked with 5% skim milk in PBS-T for 1 h at room temperature and then incubated with primary antibodies against CASP3 and β-actin at 4 °C overnight. After washing the protein blots with PBS-T, they were incubated with secondary antibodies at room temperature for 1 h. The positive bands in the blots were detected with an enhanced chemiluminescence reagent (Thermo Scientific,

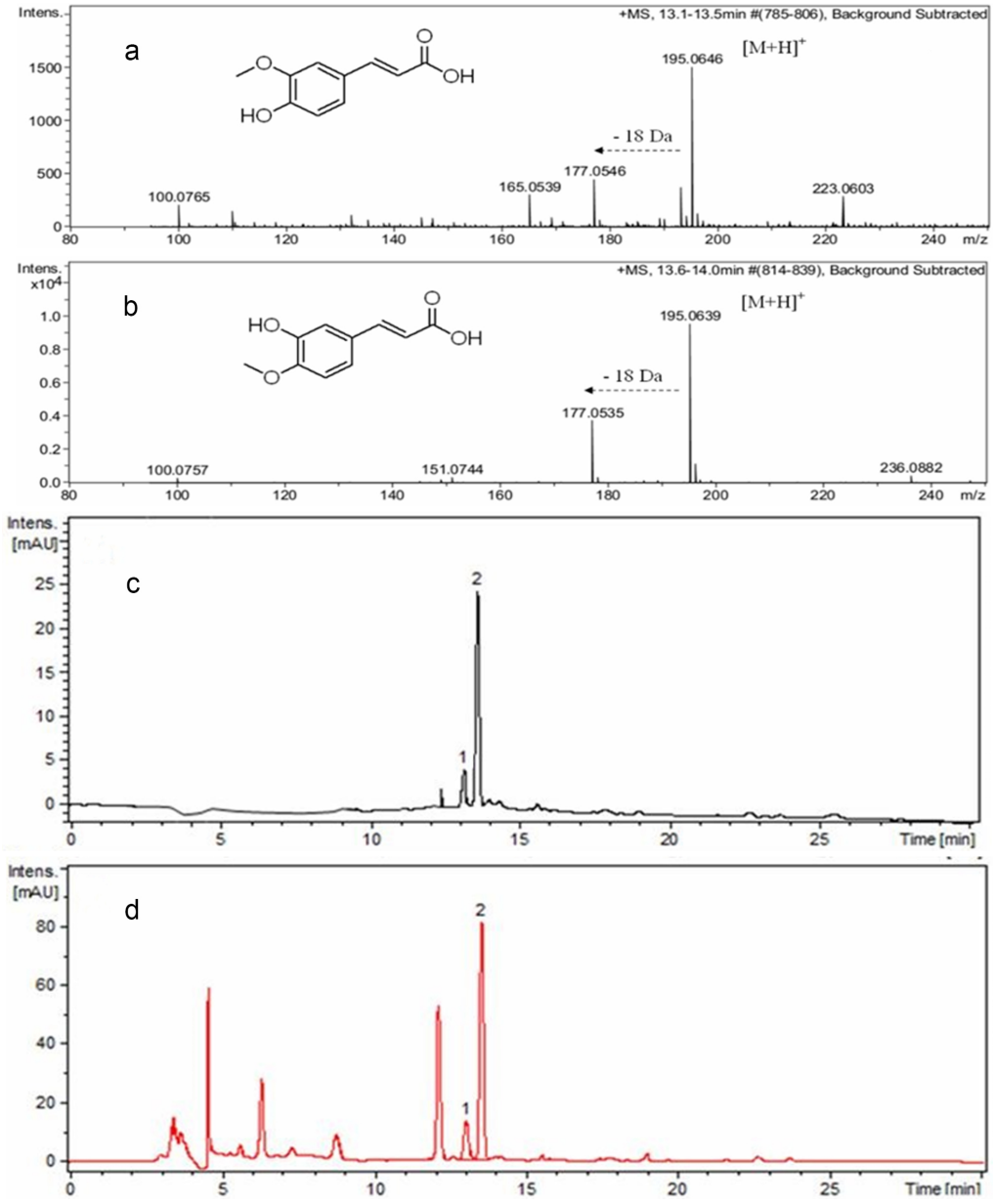

Fig. 2. Positive MS^2 spectra and Chromatographic profil for two compounds of ferulic acid and isoferulic acid. (a) Chemical structures and positive MS^2 spectra for ferulic acid and b. isoferulic acid. (b) Chemical structures and positive MS^2 spectra for isoferulic acid. (c) Blank serum spiked with reference standards of ferulic acid and isoferulic acid. (d) LCD-treated rat serum samples: (1) ferulic acid (2) isoferulic acid.

Waltham, MA, USA). The relative intensities of the protein bands were measured, and β-actin was used as an internal standard control.

2.4.8 Statistical analysis

The results are presented as the means ± standard deviations and were analysed using GraphPad Prism 5. One-way ANOVA was used to determine the statistical significance of differences between the values of various experimental groups.

3. Results

3.1 Predicting the Mechanism of LCD in Treating SLE

To screen the potential targets of LCD treating SLE, we used network pharmacology technology. All components of LCD and the related potential targets were collected from TCMSP database as shown in **Supplementary Tables 1,2**. 283 potential targets of LCD, 1498 SLE related targets and 150 common targets were obtained from 5 kinds of database using network-based method shown in Fig. 1a. We further constructed PPI networks with 150 overlapping targets between targets obtained from LCD effective com-

Table 2. The regression equation, correlation coefficient (n = 5).

Standard compounds	Linear range (μg/mL)	Regression equation	Correlation coefficient
Ferulic acid	0.15∼15.00	$y = 373895.4453x - 21277.8268$	0.9999
Isoferulic acid	0.25∼25.00	$y = 31949.5905x - 87446.3771$	0.9994

ponents and SLE disease targets. The targets were selected (combine score $\geq$0.4) by degree value using STRING 11.5 database. We installed CytoHubba plugin, screened the targets according to degree, Maximum Neighborhood Component (MNC), BottleNeck, Betweenness, etc and further visualized them using Cytoscape 3.7.1. software (Fig. 1b) [23]. The top 30 targets are ranked by degree (>140) and MNC (>70) as shown in **Supplementary Table 3**. AKT1, TNF, IL6, VEGFA, TP53, IL1B, JUN and CASP3 are key effective targets. KEGG pathway enrichment analysis of potential targets of LCD treating SLE were performed using Metascape database and the top 20 KEGG pathways were shown in Fig. 1c. LCD in the treatment of SLE enriched with pathways in cancer, AGE-RAGE signaling pathway in diabetic complications and IL-17 signaling pathway, which all related to the key target CASP3. Among these potential pathways, pathways in cancer is the most significantly enriched pathway with the smallest p value (Log10 (P) = –59.14) of the top 20 remarkable enrichment pathways.

3.2 Validation of LCD Treating SLE

3.2.1 Main Components in LCD Serum by HPLC-MS

To further predict CASP3 target of LCD treating SLE, we integrated HPLC-MS analysis with molecular docking. Different doses of LCD treated serum were prepared and identified with HPLC/MS analysis. According to the conditions described above, two components of ferulic acid (Fig. 2a) and isoferulic acid (Fig. 2b) in LCD serum were tentatively identified and showed better sensitivity in the positive ESI-MS analysis (**Supplementary Table 4**), which yielded protonated molecules at m/z 195. Based on comparisons of blank serum spiked reference standards (Fig. 2c) and LCD treated serum samples (Fig. 2d), we further performed a quantitative analysis including accuracy and precision. The linear-regression line of standards was shown in Table 2. Under the analytical conditions, the results of accuracy, intra-day precision and inter-day precision were shown in **Supplementary Table 5**. The specificity of the method was further supported based on the comparisons of chromatograms, retention times and reference standards. Based on the linear regression curves of standards, the contents of ferulic acid in high, middle and low doses of LCD serum (H, M and L) were 10.18 $\pm$ 0.36 μg/mL, 6.41 $\pm$ 0.25 μg/mL, and 5.88 $\pm$ 0.16 μg/mL and the contents of isoferulic acid were 42.23 $\pm$ 0.96 μg/mL, 34.28 $\pm$ 0.66 μg/mL, and 27.56 $\pm$ 0.46 μg/mL, respectively. A high dose of LCD serum (H) contained significantly higher amounts of ferulic acid and isoferulic acid than a middle dose (M) or a low dose (L).

3.2.2 Molecular Docking between CASP3 and Main Components from LCD

Molecular docking combined with molecular dynamics simulation were employed to reveal the detailed interactions between main compounds and potential protein targets. The potential target CASP3 with high degree and its main compounds of ferulic acid and isoferulic acid were selected for molecular docking based on the above results. Binding energies between CASP3 and compounds of ferulic acid and isoferulic acid were calculated in AUTODOCK vina. The binding energy less than zero mean spontaneous binding of targets and compounds. Lower docking energy indicating a stronger binding affinity and higher docking score. The lower the energy is, the binding is stable. It is generally accepted that the binding energy less than –5.0 kcal/mol was selected as the screening criteria. As shown in Fig. 3, ferulic acid (Fig. 3a) and isoferulic acid (Fig. 3b) buried in the binding pocket of the CASP3 target protein formed by amino-acid residues based on the hydrogen and hydrophobic interactions. Both compounds of ferulic acid and isoferulic acid bind to CASP3, but their potency were different, despite their similar structures. Three key amino acids, ARG286, GLU240 and GLU324 were found in the CASP3 (PDBID:1RHJ) - ferulic acid complex. Four key amino acids, ARG179, ARG341, GLN283 and SER236 were found in the CASP3 (PDBID:1RHU) - isoferulic acid complex. The binding energies of ferulic acid and isoferulic acid compounds with CASP3 were –5.8 kcal/mol and –5.5 kcal/mol, respectively, which showed good docking affinity. The results suggested that ferulic acid and isoferulic acid exhibited certain activity and CASP3 could be considered as an effective target of LCD in the treatment of SLE. LCD might exert protective effects against SLE through inducing CASP3 activities.

3.2.3 Anti-Proliferation Effect of LCD Serum on Activated Jurkat T Cells

We activated Jurkat T cells with β-oestradiol (300 pg/mL) and treated with different doses of LCD serum (H, M and L) for 24 h to study the potential anti-proliferation effect. The cell proliferation inhibitory rate was measured with a CCK-8 assay. As shown in Fig. 4a, the absorbance of the control group at OD450 was the highest of the four groups, indicating that β-oestradiol (300 pg/mL) induced the activation of Jurkat T cells. The viability of T cells was reduced after treatment with different doses of LCD serum (H, M and L) compared with the control group ($p < 0.05$ or $p < 0.01$). The inhibition rates were 54.6 %, 42.3 % and 14.3 %, respectively, after treatment with the three doses of

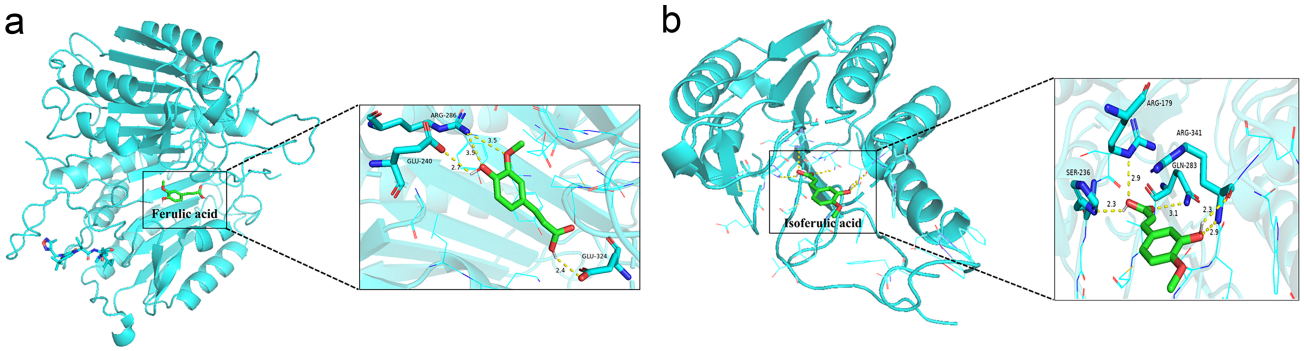

Fig. 3. The molecular docking of CASP3 target with components of ferulic acid and isoferulic acid. (a) Ferulic acid–CASP3. (b) Isoferulic acid-CASP3.

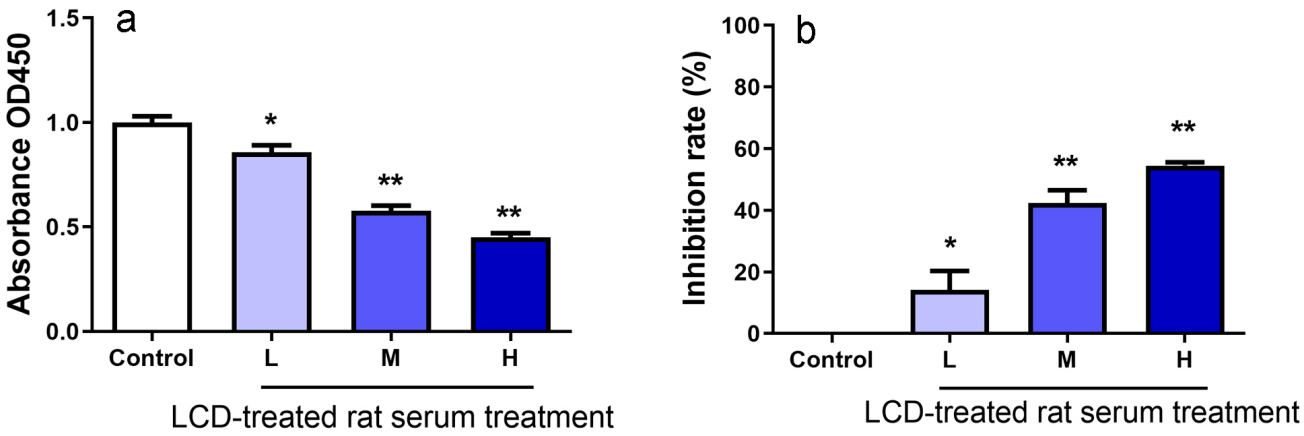

Fig. 4. Effects of LCD-treated rat serum on the inhibition rate of Jurkat T cells determined using the CCK-8 assay. Absorbance at OD450 (a) and T cell inhibition rate after treatment with different doses of LCD serum (H, M and L) (b). Values are presented as the mean ± SD. *$p < 0.05$ and **$p < 0.01$ compared with untreated control and LCD-treated cells. One-way analysis of variance (ANOVA) was used followed by Dunnett's tests (n = 3).

LCD serum (H, M and L) as shown in Fig. 4b. The highest inhibition rate was observed after treatment with a high dose of LCD serum, 54.6 % ($p < 0.01$). Based on these results, LCD exerted an anti-proliferative effect on Jurkat T cells, which may be attributed to their apoptosis induction.

3.2.4 LCD Induced Apoptosis of Activated T Cells by Flow Cytometry

To explore whether LCD serum induced apoptosis in Jurkat T cells, we stained and detected apoptotic cells with annexin V-FITC and PI. The percentage of apoptotic cells was quantified using flow cytometry and an annexin V/PI Apoptosis Assay Kit. Very few apoptotic cells were observed in the untreated control group (Fig. 5a). In contrast, the percentage of apoptotic cells increased gradually by 6.8%, 16.5% and 26.8% (Fig. 5b–d) after treatment with different doses of LCD serum (L, M and H) along with β-oestradiol (300 pg/mL), which were all significantly different from those of the untreated cells.

The early and late apoptosis rates increased gradually after treatment with low, middle and high doses of LCD serum (**Supplementary Fig. 1**). The increased apoptotic rates may be associated with LCD-induced apoptosis. The annexin V/PI double staining assay confirmed that LCD induces apoptosis in Jurkat T cells by initiating the apoptotic cascade.

3.2.5 LCD Induces CASP3 Activation

We detected the expression of one important apoptosis-related protein, CASP3, using western blot analysis to study the potential mechanism by which LCD induced apoptosis. CASP3 is one of the executioner caspases activated by proteolytic cleavage during apoptosis. The levels of β-actin were monitored to ensure equal loading of protein samples. As shown in Fig. 6, compared with the control group treated with β-oestradiol (300 pg/mL), treatment with different doses of LCD serum (L, M and H) along with β-oestradiol increased the expression levels of the CASP3 mRNA ($p < 0.05$, $p < 0.001$ and $p < 0.001$). Similarly, LCD serum (L, M and H) upregulated CASP3 protein levels ($p < 0.05$, $p < 0.001$ and $p < 0.001$). The increased level of cleaved CASP3 showed that LCD induced apoptosis in Jurkat T cells.

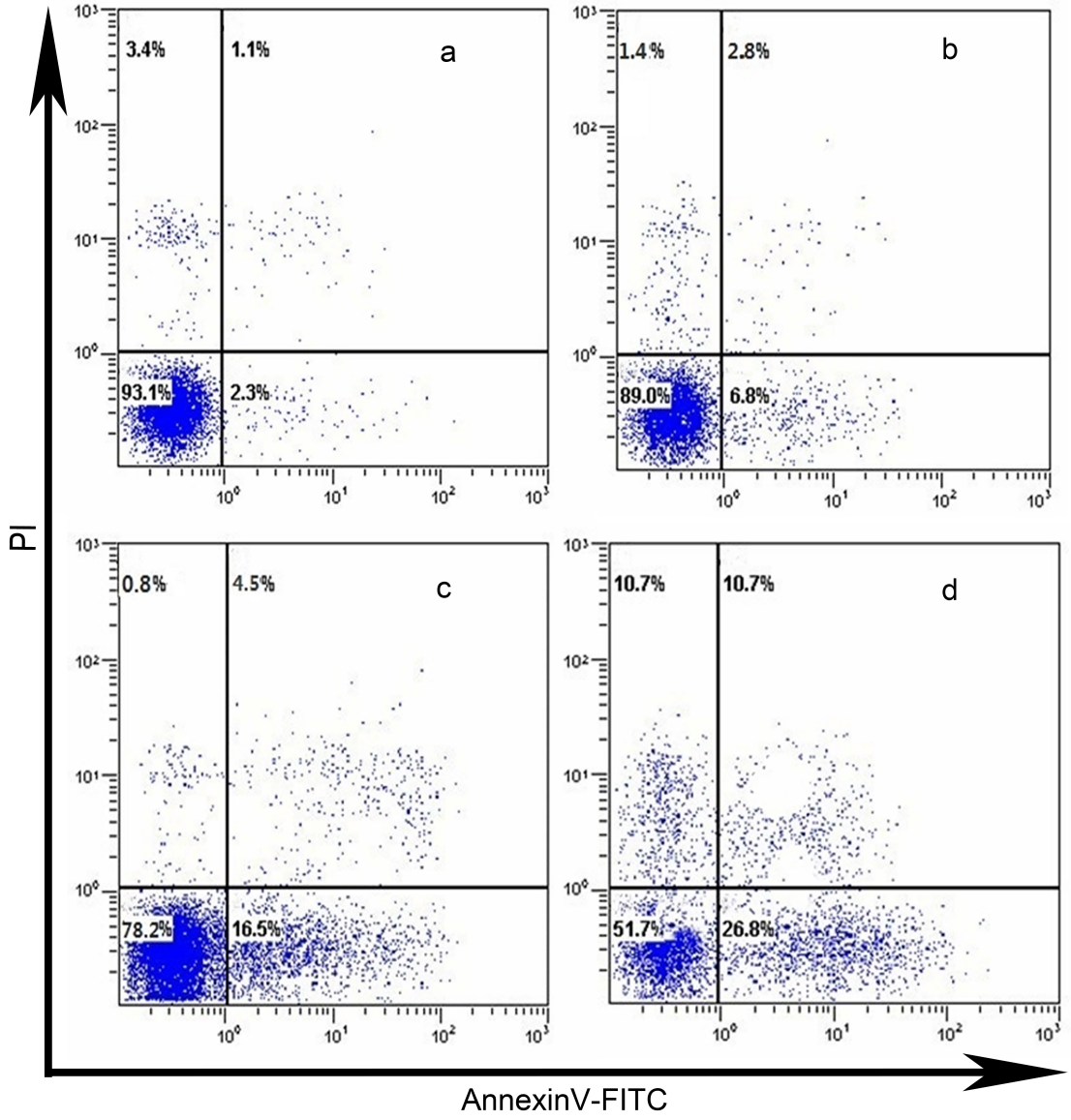

Fig. 5. Representative flow cytometry profile of Jurkat T cells treated without (a) or with low (b), middle (c) and high (d) doses of LCD-treated rat serum along with β-oestradiol (300 pg/mL) for 24 h *in vitro*. Cells were stained with annexin V/PI and then analysed on a flow cytometer. A dual-parameter dot plot of annexin V-FITC fluorescence (x axis) versus PI fluorescence (y axis) is shown in logarithmic fluorescence intensity. Quadrants: lower left indicates live cells (-FITC), lower right indicates early apoptotic cells (+FITC), and upper right indicates late apoptotic cells (+PI and +FITC).

4. Discussion

Systemic lupus erythematosus (SLE) is a chronic inflammatory autoimmune disease characterized by uncontrolled T cell activation, resulting in damage to multiple organs or systems [5,24,25]. Glucocorticoids are the main drug treatment for SLE and effectively promote the apoptosis of lymphocytes [26,27]. However, many serious effects and high recurrence rates are the main difficulties encountered in the clinic [6,8,28]. LCD, an effective TCM prescription in clinics, exerts obvious effects on treating SLE, such as alleviating SLE related clinical manifestations, reducing the SLE activity score, and improving the quality of life of patients. However, compared with modern medicine, the complex of multi-targets and mechanism in TCM hinder its acceptance and recognition in the western mainstream. Therefore, we need a well-understood method to demonstrate the effects of LCD on SLE for application to clinical popularization. In the present study, we integrated HPLC-MS analysis, network pharmacology and molecular docking approach to predict and validate the potential mechanism and target of LCD in treating SLE via suppressing activated T cells. We screened 283 protein targets from LCD and 1498 SLE - related targets from 6 kinds of database using network pharmacology. The PPI results with 150 common targets showed that CASP3 with high degree could be a key effective target.

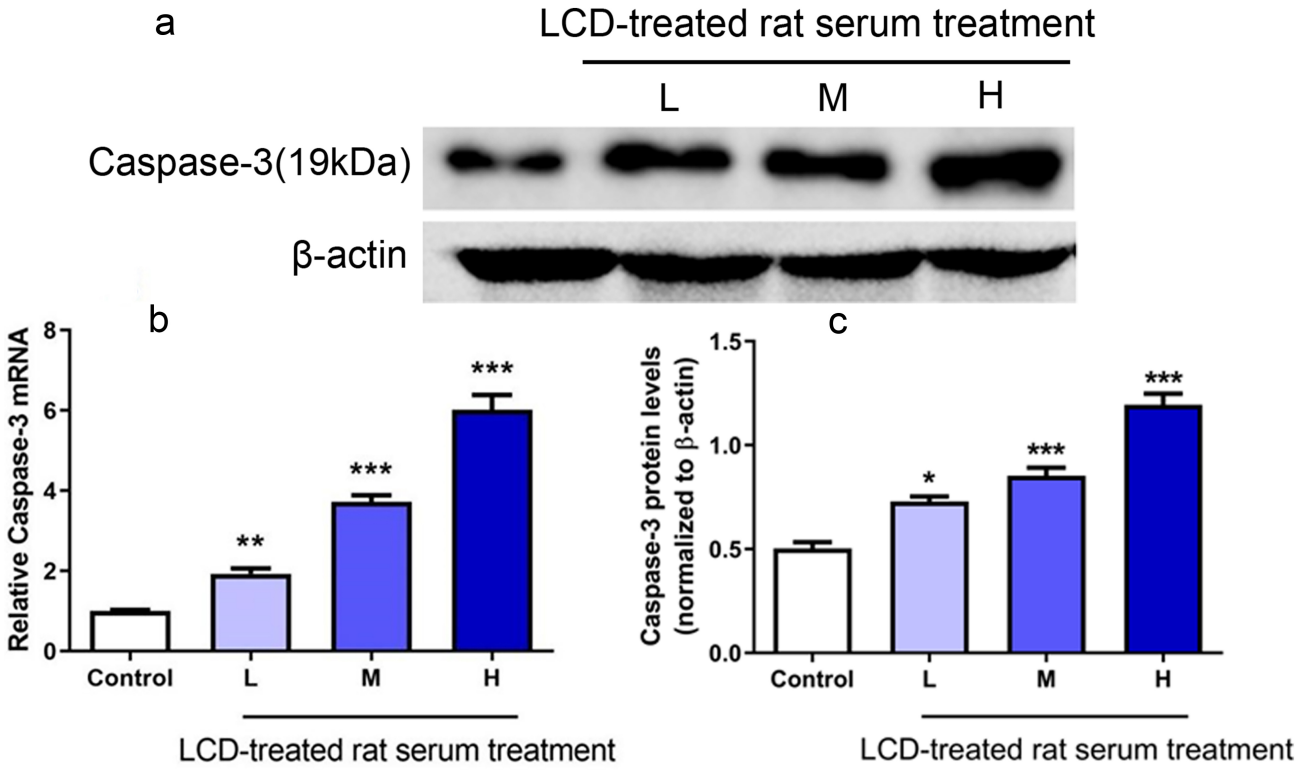

Fig. 6. Effects of LCD-treated rat serum on the caspase-3 (CASP3) mRNA and protein expression levels in Jurkat T cells. Cells were seeded in 6-well plates and treated with different doses of LCD serum (H, M and L) along with β-oestradiol (300 pg/mL) for 24 h. The protein levels were analysed using western blot analysis. β-actin was used as internal control. (a) Western blots showing levels of the β-actin and CASP3 proteins. (b) Expression level of the CASP3 mRNA. (c) Expression levels of the CASP3 protein. Values are presented as the means$\pm$ SD. $^{**}p < 0.05$, $^{**}p < 0.01$ and $^{***}p < 0.001$ compared with untreated control and LCD-treated cells. One-way analysis of variance (ANOVA) was used followed by Dunnett's test (n = 3).

Increasing evidence showed that defective control of T cells plays important roles in the pathogenesis of SLE by stimulating auto-antibody production, promoting inflammation and causing damage [3,5,29]. Apoptosis is the key process that regulates the death of activated T cells. Consequently, aberrations in T cell apoptosis are responsible for the progression of SLE. Oestrogen triggers SLE activity, which correlates with a defect in T cell apoptosis [30,31]. Therefore, to simulate the pathogenesis of SLE in the current study, we used β-oestradiol induced Jurkat cells *in vitro* as control activated T cells and further investigated the effects of LCD on activated T cells to reveal the mechanism of LCD treating SLE in the current study. Moreover, we used LCD rat serum rather than LCD to treat T cells considering that LCD rat serum is more available than human medicated serum and less interference than LCD. Different doses of LCD serum inhibited the proliferation of activated T cells by up-regulating the expression levels of the CASP3 mRNA and protein. The results confirmed that LCD might exert protective effects in the treatment of SLE by inducing apoptosis of activated T cells through initiating the activation of CASP3, which means that our prediction is appropriate and reliable.

The LCD formula is composed of *Radix Rehmanniae*, *Rhizoma Cimicifugae*, *Semen Coicis*, etc. Due to the diversity of chemical constituents and the complexity of Traditional Chinese Medicine (TCM) formula, it is difficult to assess which components contribute to therapeutic effects. Chemical composition of the prescription are the main problems of an empirical LCD formula for the treatment of SLE. In our previous report, we identified three main components from LCD, which are ferulic acid, isoferulic acid and paeoniflorin, respectively with RP-HPLC [32]. Serum medicinal chemistry is an effective method to screen active components of TCM formula, which could analyze the components absorbed into serum after oral administration with less interference of other components [33]. In the present study, we found that LCD serum contained ferulic acid and isoferulic acid based on the retention time, accurate molecular weight and fragment ion peaks of the reference substances. Furthermore, the contents of ferulic acid and isoferulic acid in LCD serum were relatively high and varied greatly in different doses of LCD treatment. Thus, we selected ferulic acid and isoferulic acid for molecular docking to predict the target CASP3 of LCD for treating SLE. They showed good docking affinity. Although it is

still unclear that which chemical components of LCD contribute to its inhibitory effect on the over-activated Jurkat T cells in the present study, we predicted and validated the potential mechanism of LCD formula in the treatment of SLE through initiating CASP3 activation for the first time. Some studies have shown that ferulic acid and isoferulic acid exert anti-inflammatory, antioxidant and apoptosis effects, consistent with our results. Our previous studies showed that LCD formula could exert obvious therapeutic effect in treating SLE patients and suppresses inflammatory activity of MRL/lpr Mice [12,13,34–36]. The present study aimed to explore the target of LCD for treating SLE via suppressing activated T cells. In the further research, we would identified more active compounds and proved the mechanism by animal model.

5. Conclusions

In conclusion, we revealed the potential mechanism of LCD formula in treating SLE via suppressing activated T cells integrating network pharmacology with HPLC-MS analysis and molecular docking. Based on a systematic prediction and experimental validation, LCD exerts an inhibitory effect on the proliferation of activated T cells in the treatment of SLE, which is potentially attributed to inducing activated T cells apoptosis by initiating CASP3 activation. LCD may be a promising choice for SLE supplementation treatment and its target CASP3 is worthy of in-depth study in our future research.

Author Contributions

HLv drafted the manuscript. HLv, QL, JS, JT, HLi, JZ, HG and ZX, were responsible for the acquisition and analysis of data. ZX and HLv were responsible for the design and supervision of the work. All authors have read and approved the final version of the manuscript.

Ethics Approval and Consent to Participate

All animals were humanely cared in Zhejiang Chinese Medical University [SCXK (Yu)-2014-0005, Zhejiang Province, P.R. China]. The study was guided and approved by Animal Ethical and Welfare Committee of ZCMU.

Acknowledgment

We appreciate the experimental support from the Public Platform of Medical Research Center and the Public Platform of Pharmaceutical Research Center, Academy of Chinese Medical, Academy of Chinese Medical Science, Zhejiang Chinese Medical University.

Funding

This research was supported by grants from the National Natural Science Foundation of China (81973829, 81873266), the Key Supported Projects of the Joint Fund of the National Natural Science Foundation of China (U21A20402) and the Natural Science Foundation of Zhejiang Province (LY18H270014).

Conflict of Interest

The authors declare no conflict of interest.

Supplementary Material

Supplementary material associated with this article can be found, in the online version, at https://doi.org/10.31083/j.fbl2711307.

References

[1] Aringer M, Costenbader K, Daikh D, Brinks R, Mosca M, Ramsey-Goldman R, *et al*. 2019 European League Against Rheumatism/American College of Rheumatology Classification Criteria for Systemic Lupus Erythematosus. Arthritis & Rheumatology. 2019; 71: 1400–1412.

[2] Lee EE, Lee EB, Park JK, Lee EY, Song YW. Performance of the 2019 European League Against Rheumatism/American College of Rheumatology classification criteria for systemic lupus erythematosus in Asian patients: a single-centre retrospective cohort study in Korea. Clinical and Experimental Rheumatology. 2020; 38: 1075–1079.

[3] Zhou H, Li B, Li J, Wu T, Jin X, Yuan R, *et al*. Dysregulated T Cell Activation and Aberrant Cytokine Expression Profile in Systemic Lupus Erythematosus. Mediators of Inflammation. 2019; 2019: 8450947.

[4] Liu Q, Deng Y, Li C, Xie H, Liu Q, Ming S, *et al*. LncRNA GAS5 suppresses CD4(+) T cell activation by upregulating E4BP4 via inhibiting miR-92a-3p in systemic lupus erythematosus. Immunology Letters. 2020; 227: 41–47.

[5] Chen J, Peng L, Zhao Z, Yang Q, Yin F, Liu M, *et al*. HDAC1 potentiates CD4 + T cell activation by inhibiting miR-124 and promoting IRF1 in systemic lupus erythematosus. Cellular Immunology. 2021; 362: 104284.

[6] Apostolopoulos D, Morand EF. It hasn't gone away: the problem of glucocorticoid use in lupus remains. Rheumatology. 2017; 56: i114–i122.

[7] Porta S, Danza A, Arias Saavedra M, Carlomagno A, Goizueta MC, Vivero F, *et al*. Glucocorticoids in Systemic Lupus Erythematosus. Ten Questions and Some Issues. Journal of Clinical Medicine. 2020; 9: 2709.

[8] Gergianaki I, Bortoluzzi A, Bertsias G. Update on the epidemiology, risk factors, and disease outcomes of systemic lupus erythematosus. Best Practice & Research: Clinical Rheumatology. 2018; 32: 188–205.

[9] Tanaka Y, O'Neill S, Li M, Tsai IC, Yang YW. Systemic Lupus Erythematosus: Targeted literature review of the epidemiology, current treatment, and disease burden in the Asia Pacific region. Arthritis Care & Research. 2022; 74: 187–198.

[10] Ma YC, Lin CC, Li CI, Chiang JH, Li TC, Lin JG. Traditional Chinese medicine therapy improves the survival of systemic lupus erythematosus patients. Seminars in Arthritis and Rheumatism. 2016; 45: 596–603.

[11] Dai L, Chan KK, Mao JC, Tian Y, Gu JH, Zhou J, *et al*. Modified Zhibai Dihuang pill, a traditional Chinese medicine formula, on steroid withdrawal in systemic lupus erythematosus: A systematic review and meta-analysis. Journal of Integrative Medicine. 2020; 18: 478–491.

[12] Shui B, Xia W, Wen C, Ding X. Jieduquyuziyin prescription suppresses IL-17 production and Th17 activity in MRL/lpr mice by inhibiting expression of Ca(2+)/calmodulin-dependent protein kinase-4. Journal of Natural Medicines. 2015; 69: 349–357.

[13] Zhang L, Sun J, Shen J, Yang YQ, He YJ, Fan YS, *et al*. Regulating Effects of Langchuangding on the Apoptosis and Expressions of GRa of CD4 +T Cells in SLE. Journal of Zhejiang Chinese Medical University. 2016; 40: 423–430. (In Chinese)
[14] Gao Y, Wang KX, Wang P, Li X, Chen JJ, Zhou BY, *et al*. A Novel Network Pharmacology Strategy to Decode Mechanism of Lang Chuang Wan in Treating Systemic Lupus Erythematosus. Frontiers in Pharmacology. 2020; 11: 512877.
[15] Zhou W, Lai X, Wang X, Yao X, Wang W, Li S. Network pharmacology to explore the anti-inflammatory mechanism of Xuebijing in the treatment of sepsis. Phytomedicine. 2021; 85: 153543.
[16] Li X, Tian G, Xu L, Sun L, Tao R, Zhang S, *et al*. Wenxin Keli for the Treatment of Arrhythmia-Systems Pharmacology and In Vivo Pharmacological Assessment. Frontiers in Pharmacology. 2021; 12: 704622.
[17] Zhang YZ, Yang JY, Wu RX, Fang C, Lu H, Li HC, *et al*. Network Pharmacology-Based Identification of Key Mechanisms of Xihuang Pill in the Treatment of Triple-Negative Breast Cancer Stem Cells. Frontiers in Pharmacology. 2021; 12: 714628.
[18] Zhou S, Ai Z, Li W, You P, Wu C, Li L, *et al*. Deciphering the Pharmacological Mechanisms of Taohe-Chengqi Decoction Extract Against Renal Fibrosis Through Integrating Network Pharmacology and Experimental Validation In Vitro and In Vivo. Frontiers in Pharmacology. 2020; 11: 425.
[19] Rose PW, Prlic A, Altunkaya A, Bi C, Bradley AR, Christie CH, *et al*. The RCSB protein data bank: integrative view of protein, gene and 3D structural information. Nucleic Acids Research. 2017; 45: D271–D281.
[20] Trott O, Olson AJ. AutoDock Vina: improving the speed and accuracy of docking with a new scoring function, efficient optimization, and multithreading. Journal of Computational Chemistry. 2010; 31: 455–461.
[21] Nozhat Z, Khalaji MS, Hedayati M, Kia SK. Different Methods for Cell Viability and Proliferation Assay: Essential Tools in Pharmaceutical Studies. Anti-Cancer Agents in Medicinal Chemistry. 2022; 22: 703–712.
[22] Ji L, Hou X, Deng X, Fan X, Zhuang A, Zhang X, *et al*. Jieduquyuziyin Prescription-Treated Rat Serum Suppresses Activation of Peritoneal Macrophages in MRL/Lpr Lupus Mice by Inhibiting IRAK1 Signaling Pathway. Evidence-Based Complementary and Alternative Medicine. 2019; 2019: 2357217.
[23] Chin CH, Chen SH, Wu HH, Ho CW, Ko MT, Lin CY. cytoHubba: identifying hub objects and sub-networks from complex interactome. BMC Systems Biology. 2014; 8: S11.
[24] Pan L, Lu MP, Wang JH, Xu M, Yang SR. Immunological pathogenesis and treatment of systemic lupus erythematosus. World Journal of Pediatrics 2020; 16: 19–30.
[25] Nusbaum JS, Mirza I, Shum J, Freilich RW, Cohen RE, Pillinger MH, *et al*. Sex Differences in Systemic Lupus Erythematosus: Epidemiology, Clinical Considerations, and Disease Pathogenesis. Mayo Clinic Proceedings. 2020; 95: 384–394.
[26] Deng J, Chalhoub NE, Sherwin CM, Li C, Brunner HI. Glucocorticoids pharmacology and their application in the treatment of childhood-onset systemic lupus erythematosus. Seminars in Arthritis and Rheumatism. 2019; 49: 251–259.
[27] Ruiz-Arruza I, Lozano J, Cabezas-Rodriguez I, Medina JA, Ugarte A, Erdozain JG, *et al*. Restrictive Use of Oral Glucocorticoids in Systemic Lupus Erythematosus and Prevention of Damage Without Worsening Long-Term Disease Control: An Observational Study. Arthritis Care & Research. 2018; 70: 582–591.
[28] Conti F, Ceccarelli F, Perricone C, Leccese I, Massaro L, Pacucci VA, *et al*. The chronic damage in systemic lupus erythematosus is driven by flares, glucocorticoids and antiphospholipid antibodies: results from a monocentric cohort. Lupus. 2016; 25: 719–726.
[29] Chen PM, Tsokos GC. T Cell Abnormalities in the Pathogenesis of Systemic Lupus Erythematosus: an Update. Current Rheumatology Reports. 2021; 23: 12.
[30] Kim WU, Min SY, Hwang SH, Yoo SA, Kim KJ, Cho CS. Effect of oestrogen on T cell apoptosis in patients with systemic lupus erythematosus. Clinical & Experimental Immunology. 2010; 161: 453–458.
[31] SongnuanBoonsoongnern P, Faisaikarm T, Sangsuwan P, Weerachatyanukul W, Kitiyanant Y. A role of oestrogen in aggravating SLE-like syndrome in C4-deficient mice. Asian Pacific Journal of Allergy and Immunology. 2015; 33: 339–348.
[32] Lv H, Zhang X, Tu J, LI Z, Wen CP. Simultaneous determination of ferulic Acid, isoferulic acid and paeoniflorin in Jiedu Quyu Ziyin recipe by dual wavelength RP-HPLC. Chinese Archives of Traditional Chinese Medicine. 2013; 31: 1245–1247. (In Chinese)
[33] Han Y, Sun H, Zhang A, Yan G, Wang XJ. Chinmedomics, a new strategy for evaluating the therapeutic efficacy of herbal medicines. Pharmacology & Therapeutics. 2020; 216: 107680.
[34] Sun J, Shao TJ, Zhang DY, Huang XQ, Xie ZJ, Wen CP. Effect of Lang-Chuang-Ding Decoction () on DNA Methylation of CD70 Gene Promoter in Peripheral Blood Mononuclear Cells of Female Patients with Systemic Lupus Erythematosus. Chinese Journal of Integrative Medicine. 2018; 24: 348–352.
[35] Ji L, Fan X, Hou X, Fu D, Bao J, Zhuang A, *et al*. Jieduquyuziyin Prescription Suppresses Inflammatory Activity of MRL/lpr Mice and Their Bone Marrow-Derived Macrophages via Inhibiting Expression of IRAK1-NF-kappaB Signaling Pathway. Frontiers in Pharmacology. 2020; 11: 1049.
[36] Hu J-b, Jiang F-s, Gu H-c, Ding Z-s, Yao L, Fan Y-s, *et al*. Metabolomics Study on the Effects of Jieduquyuziyin Prescription on Systemic Lupus Erythematosus Mice by LC-Q-TOF/MS. Chromatographia. 2013; 76: 791–800.